

**Nonlinear Rayleigh–Taylor Growth of 3-D Laser-Imprinted Modulations:**

Nonlinear growth of 3-D broadband nonuniformities was measured near saturation levels using x-ray radiography in planar foils accelerated by laser light. In the experiments, 20- and 50- $\mu\text{m}$ -thick planar CH targets were driven with 12-ns square pulses at a laser intensity of  $\sim 5 \times 10^{13} \text{ W/cm}^2$  on the OMEGA laser system. The modulation growth was measured with through-foil, x-ray radiography using x rays from three different backlighters [1.3 keV (U), 2.0 keV (Dy), and  $\sim 2.5 \text{ keV}$  (Ta)]. The initial target modulations were imprinted by laser-intensity nonuniformities of the imprinting beam, a separate beam that arrived  $\sim 200 \text{ ps}$  before the drive beams that were used to accelerate the target. Two different initial target modulations were created by the imprinting laser beam using either a standard distributed phase plate (SG8 DPP) or no DPP with the beam defocused to an  $\sim 1\text{-mm}$  spot. Figure 1 shows measured, central,  $333\text{-}\mu\text{m}$ -sq parts of the laser equivalent-target-plane images with SG 8 DPP (a) and no DPP (b). The laser-modulation Fourier spectra of these laser images are shown in Fig. 1(c). The beam with DPP (blue) has broadband modulations with spatial frequencies up to  $\sim 320 \text{ mm}^{-1}$ , corresponding to the smallest spatial size of  $\sim 3 \mu\text{m}$ . The beam with no DPP (red) has modulations with spatial frequencies up to  $\sim 50 \text{ mm}^{-1}$ . The processed time-gated images of the x-ray radiographs are compared in Fig. 2 for these two cases.

Figure 3 summarizes the growth results. The dashed line in Fig. 3(a) shows the growth rate  $\gamma(k)^1$  as a function of spatial frequency. The diamonds correspond to the measured growth rates of 120- and 60- $\mu\text{m}$ -wavelength modulations from all shots (with initial conditions including both SG8 DPP and no DPP). The dashed line in Fig. 3(b) shows the saturation velocity  $V_s(k) = S_k \gamma(k)$  as a function of spatial frequency, where  $S_k = 2/Lk^2$  is the saturation level, as defined by the Haan model.<sup>1</sup> The measured saturation velocities are in excellent agreement with Haan model<sup>1</sup> predictions. Once the modulations enter the nonlinear regime, the velocities do not depend on initial conditions. The measured growth rates of long-wavelength modulations are higher (by about a factor of 2) than the Haan-model predictions (given by the Betti–Goncharov formula<sup>2</sup>). A recent study<sup>3</sup> by Sanz *et al.* predicted enhanced mode-coupling to longer-wavelength modes in the ablative RT instability, compared to the classical RT case. The present experiments are consistent with this new study.

**OMEGA Operations Summary:** During March 2005, OMEGA conducted a total of 131 target shots for LLE, LLNL, and SNL experiments as follows: 92 shots were taken for the LLE ISE, Astro, and RTI campaigns; 34 shots were dedicated to LLNL-led campaigns, and 5 target shots were conducted for SNL experiments. In addition, planned quarterly maintenance activity was carried out in the last week of the month.

1. S. W. Haan, Phys. Rev. A **39**, 5812 (1989).  
 2. R. Betti *et al.*, Phys. Plasmas **5**, 1446 (1998).  
 3. J. Sanz *et al.*, Phys. Rev. Lett. **89**, 195002 (2002).

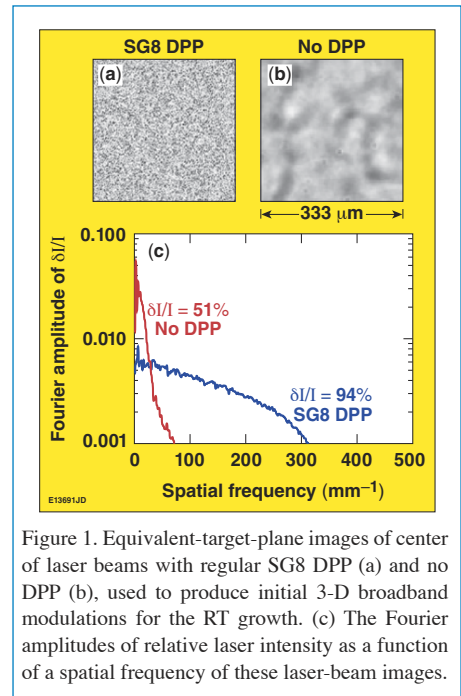


Figure 1. Equivalent-target-plane images of center of laser beams with regular SG8 DPP (a) and no DPP (b), used to produce initial 3-D broadband modulations for the RT growth. (c) The Fourier amplitudes of relative laser intensity as a function of a spatial frequency of these laser-beam images.

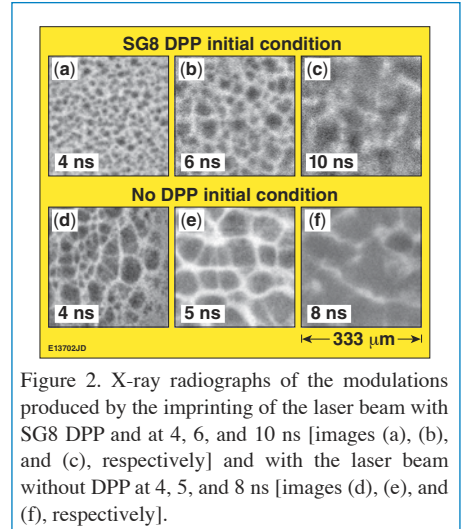


Figure 2. X-ray radiographs of the modulations produced by the imprinting of the laser beam with SG8 DPP and at 4, 6, and 10 ns [images (a), (b), and (c), respectively] and with the laser beam without DPP at 4, 5, and 8 ns [images (d), (e), and (f), respectively].

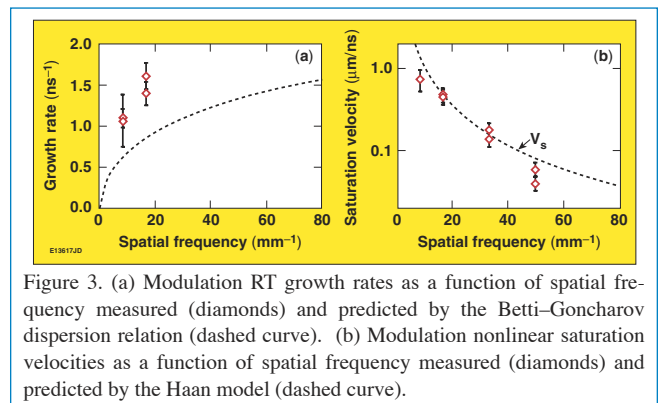


Figure 3. (a) Modulation RT growth rates as a function of spatial frequency measured (diamonds) and predicted by the Betti–Goncharov dispersion relation (dashed curve). (b) Modulation nonlinear saturation velocities as a function of spatial frequency measured (diamonds) and predicted by the Haan model (dashed curve).